Available on CMS information server **CMS NOTE 2006/096**

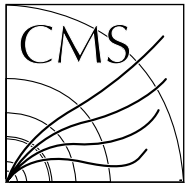

The Compact Muon Solenoid Experiment

CMS Note

Mailing address: CMS CERN, CH-1211 GENEVA 23, Switzerland

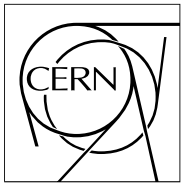

July 20, 2006

Search for $\tilde{\chi}_2^0$ decays to $\tilde{\tau}\tau$ and SUSY mass spectrum measurement using di-τ final states.

D. J. Mangeol, U. Goerlach

IPHC, Strasbourg, France

Abstract

The SUSY discovery potential at CMS is investigated during the low luminosity $2 \cdot 10^{33} cm^2 s^{-1}$ running phase of the LHC. The study focuses on the cascade decay chain $\tilde{q} \rightarrow q\tilde{\chi}_2^0 \rightarrow q\tau\tilde{\tau} \rightarrow q\tau\tau\tilde{\chi}_1^0$. It shows that low mass SUSY can be discovered in di-τ final states with only few hundreds pb^{-1}. The measurement of the mass spectrum is also performed with a kinematic end-point technique applied for the first time to hadronic τ's.

1 Introduction

In proton-proton collisions, SUSY is mainly produced through $\tilde{q}$ and $\tilde{g}$ pair production. The $\tilde{q}$ and $\tilde{g}$ eventually decay to the lightest supersymmetric particle (LSP) through cascade decays of variable "length". In R-parity conserving models such as the ones examined in this note, the LSP is the lightest $\tilde{\chi}^0$ which is weakly interacting and escapes detection. Consequently, a direct measurement of the masses of the sparticle cannot be performed. However, among the various cascades, those of the type $\tilde{q} \rightarrow q\tilde{\chi}_2^0$ are particularly interesting as the $\tilde{\chi}_2^0$ two-body decays followed by slepton two-body decays offer a system that is kinematically constrained. This one can be solved using kinematic edge measurements, hence allowing access to the sparticle masses.

In this note, the cascade decay $\tilde{q} \rightarrow q\tilde{\chi}_2^0 \rightarrow q\tau\tilde{\tau} \rightarrow q\tau\tau\tilde{\chi}_1^0$ is investigated in the context of mSUGRA [1]. In this particular case, the decay process involves the production of the $\tilde{\tau}$. At low $\tan\beta$, the branching fraction of the $\tilde{\chi}_2^0$ decaying into $\tilde{\tau}$ is of the same order as the other sleptons while at large $\tan\beta$, this one becomes predominant reaching 96% at $\tan\beta$=35. It is therefore important to be able to study $\tilde{\tau}$ production as it might extend the reach for SUSY to large $\tan\beta$ or to constraint mSUGRA if $\tan\beta$ is smaller. However, the presence of ν_τ in the decay products of the τ-lepton largely complicates the study and the reconstruction of this cascade decay.

The analysis is first performed at the LM2 test point ($m_0 = 185$ GeV, $m_{1/2} = 350$ GeV, $A_0 = 0$, $\tan\beta$=35 and $\mu > 0$) where the branching ratio $\tilde{\chi}_2^0 \rightarrow \tau\tilde{\tau}$ is close to 96%. That point was also chosen compatible with WMAP and is nearly identical to point I' described in [2]. The various CMS test points in the $(m_0, m_{1/2})$ plane are shown in figure 1. The SUSY discovery potential using this analysis is assessed over the $(m_0, m_{1/2})$ plane for different accumulated luminosity values.

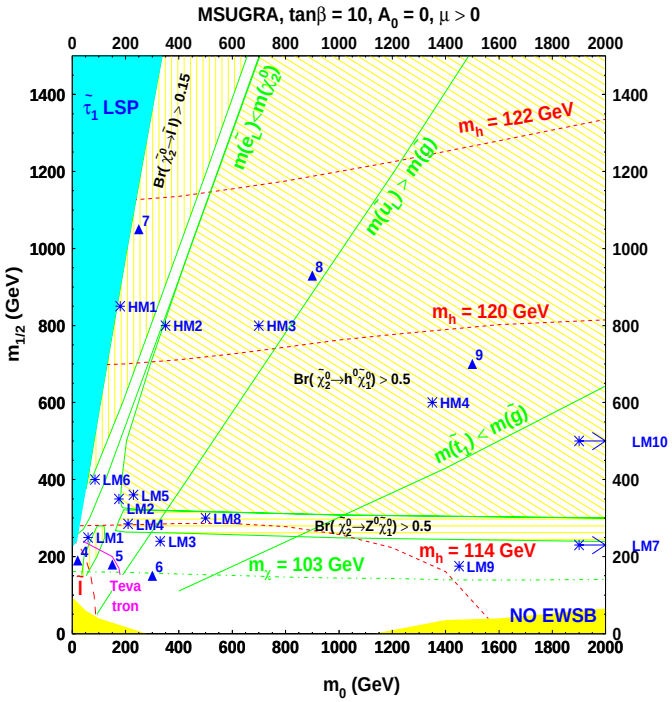

Figure 1: Position of the CMS test points in the $(m_0, m_{1/2})$ plane

This note is organized as follows. Section 2 describes the event reconstruction and selection procedure. In section 3, the possibility of finding mSUGRA with di-τ analysis is presented and discussed. Finally, the end-point extraction technique and SUSY mass spectrum measurement using hadronic di-τ's are presented in section 4.

2 Selection procedure

For this study, the signal dataset was generated with CTEQ 5L [3] Leading Order PDF set using ISAJET 7.69 [4] and PYTHIA 6.225 [5] at the LM2 test point, resulting in a cross section of 7.38 pb. The generated sample was simulated using the detailed GEANT4 based CMS simulation package (OSCAR [6]) then reconstructed with the

CMS reconstruction package (ORCA [7]). The Standard Model physics background samples used in this analysis were processed as well with the OSCAR-ORCA simulation-reconstruction chain. For the discovery survey of the mSUGRA parameter space, the CMS fast simulation and reconstruction package FAMOS [8] was used.

The experimental signature of $\tilde{q} \rightarrow q\tilde{\chi}_2^0 \rightarrow q\tau\tilde{\tau} \rightarrow q\tau^{\pm}\tau^{\mp}\tilde{\chi}_1^0$ is characterized by a large $E_{\mathrm{T}}^{\mathrm{miss}}$ due to the two undetected $\tilde{\chi}_1^0$ (one for each cascade) and the neutrinos produced by the τ decays, several high energy quark jets which number varies depending on how the $\tilde{q}$ is produced (directly or through the decay of the $\tilde{g}$) and a minimum of two τ's.

2.1 Event reconstruction

2.1.1 jet reconstruction and $E_{\mathrm{T}}^{\mathrm{miss}}$

Jet candidates are reconstructed with the simple iterative cone based algorithm [9] with a cone size of $\Delta R = \sqrt{(\Delta\phi)^2 + (\Delta\eta)^2} = 0.5$. They are calibrated using the "γ-jet" calibration [11].

The missing transverse energy ($E_{\mathrm{T}}^{\mathrm{miss}}$) is obtained from the aforementioned calibrated jets retaining those having a transverse energy higher than 15 GeV.

$$E_{\mathrm{T}}^{\mathrm{miss}} = \| - \sum_{\mathrm{jets}} \vec{E}_T \|$$

2.1.2 τ identification

The decay of the τ leads, beside the neutrinos which escape detection, to the production of a small number of particles containing most of the time a maximum of three charged particles. Among these decays 35% are from leptonic τ decays which also produce an additional neutrino, 50% are hadronic "1-prong" which contain one charged particle and several neutral particles and 15% are "3-prong" which contain three charged particles and several neutral particles. As long as the transverse energy of the τ is large compared to its mass, these particles are produced within a narrow cone and appear in the detector as a narrow jet-like structure called τ-jet (by extension, τ-jet is used in the note to refer to the detected particles produced by the decay of the τ.) At low energy, this cone becomes large. The identification of the τ uses mainly this property. τ's are searched among jet candidates having a maximum of three tracks found within a narrow cone (signal cone) and containing no particle outside that narrow cone [12]. However, at low energy, as the signal cone becomes large, the purity of the τ identification drops.

The energy of the τ's produced in the decay of $\tilde{\chi}_2^0$ to $\tau\tilde{\tau}$ is directly linked to the mass of the sparticles and depends on the mSUGRA parameter values. At the LM2 test point, the mass difference between the $\tilde{\tau}$ and the $\tilde{\chi}_1^0$ is small (around 16 GeV) resulting in the production of a low energy τ in the $\tilde{\tau}$ decay. This is shown in figure 7 which displays the generated level p_{T} of the two τ's, as well as their associated τ-jets, produced in the $\tilde{\chi}_2^0$ decay. The one produced in the decay of the $\tilde{\tau}$ is seen to have a very small p_{T}.

The identification of this τ, essential to the reconstruction of the $\tilde{\chi}_2^0$ decay chain, requires special care and has lead the following optimization of the τ reconstruction algorithm.

The τ candidates are searched among jet candidates obtained with the iterative cone algorithm with $\Delta R = 0.6$ and must survive the following requirements:

- The most energetic track (leading track) should be found in a cone smaller than $\Delta R = 0.17$ around the jet axis and have a minimum p_{T} of 5 GeV. Its transverse impact parameter should be smaller than 0.7 mm.
- Any other track must lie around the leading track within a cone smaller than $\Delta R = 0.1$ (signal cone) and have a p_{T} of at least 0.8 GeV.
- Only candidates with one or three tracks in the signal cone are kept.
- The isolation cone is defined as the ring between $\Delta R = 0.17$ and 0.4.

  For one-track τ candidates with E_{T} smaller than 60 GeV, the isolation cone may contain a maximum of one track if its p_{T} is larger than 10% of the track found in the signal cone. (This criteria is changed to 20% for higher energy τ candidates.) For three-tracks τ candidates, this isolation cone should not contain any track with p_{T} larger than 1 GeV.

The charge of the resulting τ candidates is obtained by summing over the charge of all the tracks found in the signal cone.

The efficiency and purity of the τ candidates are 17% and 66% for low p_{T} τ's ($p_{\mathrm{T}} < 60$ GeV) respectively and 59% and 63% for high energy p_{T} τ's respectively.

2.1.3 Leptonic τ decays rejection

The leptonic τ decays represent a total of 27% (21% and 6% for electronic and muonic τ decays respectively) of the reconstructed τ's. However, the contamination of the leptonic τ decay channels by any other lepton may be high in some case. Therefore, it is useful to be able to discard these decay channels from the analysis to avoid contamination from other process.

The leptonic τ decays can be discriminated from the hadronic "1-prong" by the fraction of energy of the track deposited in both electromagnetic and hadronic calorimeters, $F_{\mathrm{ECAL}} = E_T^{\mathrm{ECAL}}/P_T^{\mathrm{track}}$ and $F_{\mathrm{HCAL}} = E_T^{\mathrm{HCAL}}/P_T^{\mathrm{track}}$. For electronic τ decays, most of the energy is deposited in the ECAL and for muonic τ decays, while for the muon only small amount is deposited in the ECAL or HCAL (figure 2).

Therefore, electronic τ candidates are removed by rejecting candidates satisfying

$$0.15 < F_{\mathrm{HCAL}} < 0.4 \text{ and } 0.8 < \mathrm{F_{ECAL}} < 1.3,$$

$$F_{\mathrm{HCAL}} < 0.15 \text{ and } 0.6 < \mathrm{F_{ECAL}} < 2,$$

and muonic τ candidate are removed by rejecting τ candidates satisfying

$$F_{\mathrm{HCAL}} < 0.7 \text{ and } \mathrm{F_{ECAL}} < 0.15.$$

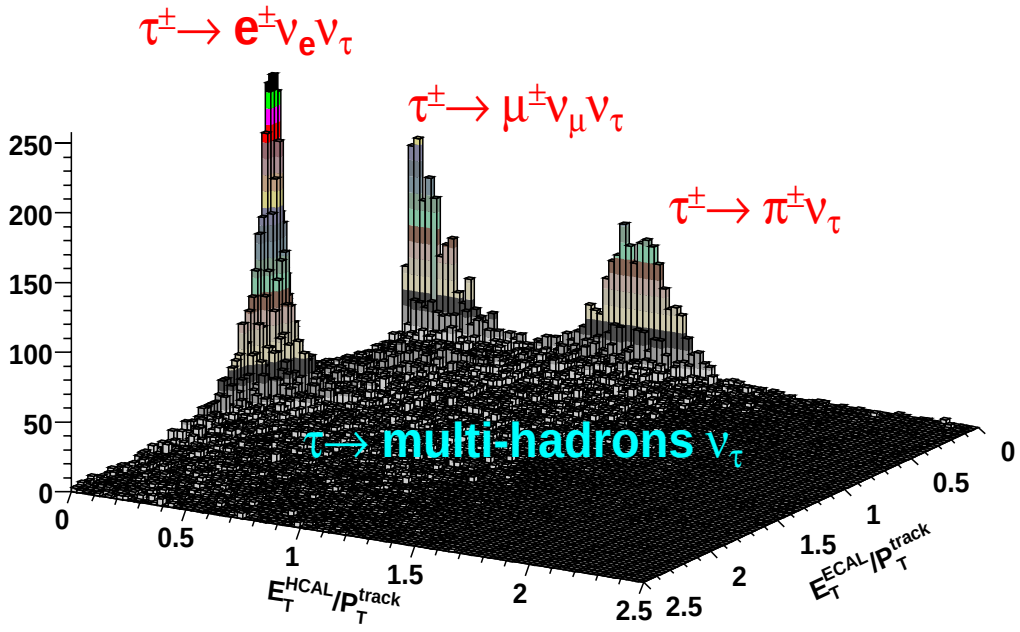

Figure 2: Fractions of the track energy deposited in the HCAL and the ECAL for "1-prong" τ decays.

2.2 Event selection

Events used in this analysis must pass both Level1 (L1) and High Level Trigger (HLT) JETMET trigger bits which require at least a single jet with an E_{T} greater than 180 GeV and missing transverse energy larger than 123 GeV. 77% of the LM2 events survive the trigger requirement.

Any physics process which can produce final states containing several τ's is considered as a potential background source. Therefore, physics processes responsible for W (hence $t\bar{t}$ also) and Z productions were thoroughly investigated as they represent the most important sources of τ's in Standard Model physics. Also, because of its huge cross section ($1.3 \cdot 10^{-4}$ mb), QCD multi-jet events represent an important source of fake tau background. These events are also an important source of fake $E_{\mathrm{T}}^{\mathrm{miss}}$ due to jet energy mismeasurements. The most important background sources used in this analysis can be found in table 1.

The signal events are selected with the following requirements:

- The missing transverse energy is required to be larger than 150 GeV.

  Since mSUGRA sparticles are pair produced and result in two cascade decays, two $\tilde{\chi}_1^0$ and several ν_τ are expected in each event. Therefore a large $E_{\mathrm{T}}^{\mathrm{miss}}$ is expected. The above requirement removes a large fraction of the Standard Model physics backgounds which have, in general, relatively low $E_{\mathrm{T}}^{\mathrm{miss}}$.

- At least two τ-jet candidates.

- At least two jets with $E_T > 150$ GeV.

  This requirement is particularly effective on $t\bar{t}$ and $W + \mathrm{jet}$ events.

- ΔR between any pair of τ's should be smaller than two.

  This requirement takes into account the property of the di-τ production originating from a same mSUGRA cascade decay. In Standard Model physics, τ's are produced more or less back to back in the plane transverse to the beam axis. While, in the $\tilde{\chi}_2^0$ cascade decays, the two τ's being produced along a same cascade, they tend to be produced relatively close to each other.

Table 1: Remaining cross section for SUSY and Standard Model physics processes after each requirement. The upper numbers correspond to the selection using all tau candidates, the underlined ones when only hadronic tau candidates are used in the selection

Physics process	no sel. (pb)	$E_{\mathrm{T}}^{\mathrm{miss}} > 150$ GeV (pb)	2 τ cand. (pb)	2 Jets$^{\mathrm{E_T}>150\ \mathrm{GeV}}$ (pb)	$\delta R(\tau,\tau) < 2$ (pb)	L1+HLT (pb)
LM2 sample	7.38	6	0.72	0.43	0.23	0.216
inclusive			<u>0.4</u>	<u>0.24</u>	<u>0.12</u>	<u>0.11</u>
LM2 sample	3.81	2.97	0.6	0.36	0.20	0.19
inclusive di-τ production			<u>0.33</u>	<u>0.2</u>	<u>0.11</u>	<u>0.10</u>
LM2 sample	2.44	1.92	0.46	0.28	0.16	0.16
$\tilde{\chi}_2^0$ cascade decay			<u>0.25</u>	<u>0.16</u>	<u>0.09</u>	<u>0.08</u>
$t\bar{t}$	492	25.8	2.6	0.12	0.045	0.029
inclusive			<u>0.8</u>	<u>0.039</u>	<u>0.014</u>	<u>0.009</u>
QCD	5930	16	0.25	0.13	0.038	0.019
$170 < \hat{p}_T < 400$ GeV			<u>0.18</u>	<u>0.1</u>	<u>0.035</u>	<u>0.019</u>
QCD	437	12	0.12	0.11	0.035	0.018
$\hat{p}_T > 400$ GeV			<u>0.09</u>	<u>0.08</u>	<u>0.025</u>	<u>0.013</u>
Wbt	0.1	0.011	0.003	0.0002	0.00003	0.000024
$W \rightarrow \tau\nu_\tau$			<u>0.002</u>	<u>0.0001</u>	<u>0.00002</u>	<u>0.000014</u>
$W + \mathrm{jets}$	263	96.1	3.2	0.042	0.0078	0.0078
$125 < \hat{p}_T < 800$ GeV			<u>0.97</u>	<u>0.015</u>	<u>0.003</u>	<u>0.003</u>
$Z/\gamma^\star \rightarrow \tau\tau$	0.2	0.03	0.006	0.0003	0.00009	0.00008
$\hat{p}_T > 300$ GeV			<u>0.005</u>	<u>0.0002</u>	<u>0.00008</u>	<u>0.00006</u>

2.3 Systematic uncertainties

The main sources of systematics considered in this analysis are coming from uncertainties in calibration and reconstruction of the various observables used in the analysis. This section reports on the impact of these uncertainties on the selection of the main Standard Model background sources.

- Contribution due to uncertainties in the jet scale [9]:

  The jet scale uncertainty is found to impact the selection of the main background sources by 13.5% in the early running period of LHC (i.e. the first fb^{-1}). For higher integrated luminosities, this uncertainties decreases and is only of 6%. The jet scale uncertainty also impacts the invariant mass measurement.

- Contribution due to uncertainties in $E_{\mathrm{T}}^{\mathrm{miss}}$ measurement [10].

  This contribution affects the selection of the background by 9% for integrated luminosities larger than 1 fb^{-1}. For the first fb^{-1}, this uncertainty is as high as 27%.

- Contribution due to uncertainties in the τ reconstruction

  The systematic uncertainty on the τ-jet energy scale has practically no effect on the selection as the number of reconstructed τ's remains unchanged. This uncertainty affects essentially the invariant mass measurement therefore only the case for integrated luminosities larger than 1 fb^{-1} were investigated.

3 Results and discovery potential

At 12.67 fb^{-1} a total of $2735 \pm 52(\mathrm{stat})$ LM2 events are expected to survive the selection for a total of $938 \pm 103(\mathrm{sys}) \pm 114(\mathrm{stat})$background events. 50% of the remaining background is coming from QCD, 39% from $t\,\bar{t}$ and 11% from W+jet (see table 1). This corresponds to a ratio signal over background, S/B, of 2.9. The global efficiency of the selection on the signal is around 3% (of which 88% are SUSY events with at least two τ's), while only 0.001% of the background remains after selection. Based on this result, a 5σ discovery could be achieved with 0.125 fb^{-1} with the S_{cp} significance [13] where both statistical and systematic uncertainties on the background are taken into account. If only statistical uncertainties are accounted for, using S_{cl} significance [14], such a discovery could even be made with only 0.07 fb^{-1}.

3.1 Event selection using only reconstructed τ's decaying hadronically

Applying the electron and muon veto described in section 2.1.3, only τ's decaying hadronically are kept in the following.

At 12.67 fb^{-1}, $N_s = 1447 \pm 38(\mathrm{stat})$ events from the signal and $N_{bkg} = 543 \pm 60(\mathrm{sys}) \pm 112(\mathrm{stat})$ events from the background survive the selection. 70% of the remaining background is coming from QCD, 20% from $t\,\bar{t}$ and 10% from W+jets. To this selection corresponds a ratio signal over background, S/B, of 2.6. The global efficiency of the selection on the signal is around 1.5%, while only 0.0006% of the background remains after selection. Using S_{cL} a 5σ discovery is achieved with only 0.14 fb^{-1}. If the systematic uncertainty on the background is also taken into account, a 5σ discovery can be expected with 0.26 fb^{-1}.

3.2 Discovery potential of mSUGRA with hadronic di-τ final states

A scan of the mSUGRA $(m_0, m_{1/2})$ plane is performed to determine the mSUGRA parameter region accessible to this analysis. The branching ratio to di-τ's and to other leptons varying with the mSUGRA parameter values, the τ reconstruction algorithm may in some cases misidentifies as τ some of the electrons and muons produced by the decay of the $\tilde{\mu}$ and $\tilde{e}$. To avoid this contamination and to concentrate on the $\tilde{\tau}$ production, the scan is performed using only hadronic τ decays as described in 3.1.

This scan is achieved by generating many mSUGRA samples varying m_0 and $m_{1/2}$ values so that the entire region of the plane $(m_0, m_{1/2})$ below $m_0 < 1500$ GeV and $m_{1/2} < 800$ GeV is covered. These samples were generated with ISAJET 7.69 and PYTHIA 6.225 then simulated and reconstructed with FAMOS and analyzed in the same way as the LM2 sample. The resulting number of events surviving the selection were used to estimate the significance at each point of the mSUGRA parameter plane. Two types of significance are estimated here, S_{cL} which accounts only for statistical effects and S_{cp} which accounts for both statistical and systematics effects on the background.

The resulting 5σ contours over mSUGRA $(m_0, m_{1/2})$ plane obtained with S_{cl} for several integrated luminosities between 0.1 and 10 fb^{-1} are shown in figures 3 and 4 for $\tan\beta = 10$ and $\tan\beta = 35$, respectively. Results obtained with S_{cp} are shown in figures 5 and 6.

The inclusive di-τ analysis allows the discovery of SUSY over a large region of the mSUGRA $(m_0, m_{1/2})$ plane, for both $\tan\beta = 10$ and 35. For large value of m_0 ($m_0 > 500$ GeV), SUSY di-τ production arises mainly from

higgs decay to $\tau\tau$ and presents similar rate for both $\tan\beta = 10$ and $\tan\beta = 35$. For low value of m_0, SUSY is discovered by $\tilde{\chi}_2^0 \to \tau\tilde{\tau}$. This process is also responsible for the large bump structures observed in the 5σ discovery contours around $m_0 = 250$ GeV for $\tan\beta = 35$. A similar structure, although much less pronounced, is also observed for $\tan\beta = 10$. The differences in shape for the 5σ discovery contours between the $\tan\beta = 10$ and $\tan\beta = 35$ plots are due to the branching ratio for $\tilde{\chi}_2^0 \to \tau\tilde{\tau}$. For $\tan\beta = 35$, the $\tilde{\chi}_2^0$ decays almost exclusively to $\tilde{\tau}$ and enhances the SUSY discovery region, while for smaller $\tan\beta$ values where the $\tilde{\chi}_2^0$ is allowed to decay to any sleptons, this enhancement is reduced.

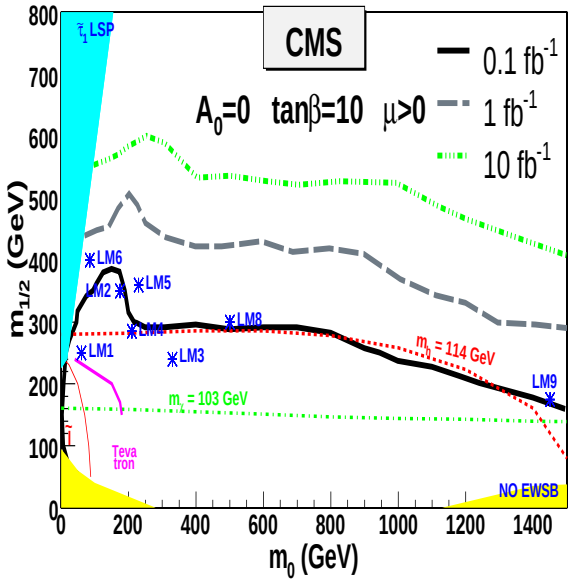

Figure 3: 5σ discovery contours for luminosities between 0.1 and 10 fb^{-1} at $\tan\beta = 10$.

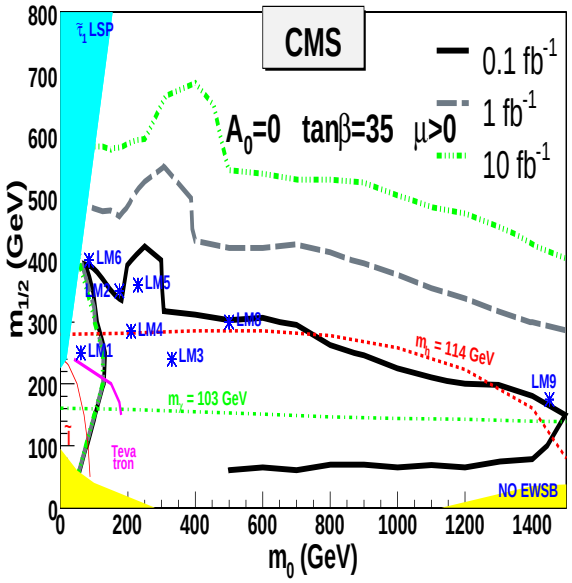

Figure 4: 5σ discovery contours for luminosities between 0.1 and 10 fb^{-1} at $\tan\beta = 35$.

4 End-point analysis and mass spectrum measurement

The cascade decay chain $\tilde{q} \to q\tilde{\chi}_2^0 \to q\tau\tilde{\tau} \to q\tau\tau\tilde{\chi}_1^0$ allows the use of the kinematic edge technique to extract the mass of the sparticles. This technique takes advantage of the three two-body decays present in the cascade to build four relations between the four sparticle masses and the end-points of the invariant mass distributions obtained by combining the quark-jet and the two τ observed in the final states.

This method has been already used to extract the SUSY mass spectrum using di-electrons and di-muons cascade decays [15], however this study is the first attempt of using it with di-τ's.

The invariant mass measured in this study are $m(\tau_1\tau_2)$, $m(\tau_1 q)$, $m(\tau_2 q)$, $m(\tau_1\tau_2 q)$ and $(m(\tau_1 q) + m(\tau_2 q))$ where τ_1 represents the τ candidate of a τ pair for which $m(\tau_1 q) > m(\tau_2 q)$. At the LM2 test point, the relation between the end-point and the sparticle masses are [15]:

$$m(\tau_1\tau_2)^{\max} = \sqrt{(M^2_{\tilde{\chi}_2^0} - M^2_{\tilde{\tau}})(M^2_{\tilde{\tau}} - M^2_{\tilde{\chi}_1^0})/M^2_{\tilde{\tau}}} \;\; ; \;\; m(\tau_1\tau_2 q)^{\max} = \sqrt{(M^2_{\tilde{q}} - M^2_{\tilde{\chi}_2^0})(M^2_{\tilde{\chi}_2^0} - M^2_{\tilde{\chi}_1^0})/M^2_{\tilde{\chi}_2^0}}$$

$$m(\tau_1 q)^{\max} = \sqrt{(M^2_{\tilde{q}} - M^2_{\tilde{\chi}_2^0})(M^2_{\tilde{\chi}_2^0} - M^2_{\tilde{\tau}})/M^2_{\tilde{\chi}_2^0}} \;\; ; \;\; m(\tau_2 q)^{\max} = \sqrt{(M^2_{\tilde{q}} - M^2_{\tilde{\chi}_2^0})(M^2_{\tilde{\tau}} - M^2_{\tilde{\chi}_1^0})/(2M^2_{\tilde{\tau}} - M^2_{\tilde{\chi}_1^0})}$$

Due to the undetected ν_τ, the invariant mass distributions obtained using τ candidates are shifted and smeared to lower values. This effect is particularly dramatic in the case of the invariant mass distribution formed by the two τ's as seen in figure 8. The invariant mass distribution made with undecayed τ's exhibits a triangle shaped distribution where the end-point coincides with the maximum of the distribution while if only the τ-jets are considered the shape of the invariant mass distribution becomes more gaussian-like with an end-point lying at the end of the tail of the distribution. Although, the position of the end-point is not changed by the loss of the information about the neutrinos, its access is difficult and requires the parametrization of the tail of that distribution.

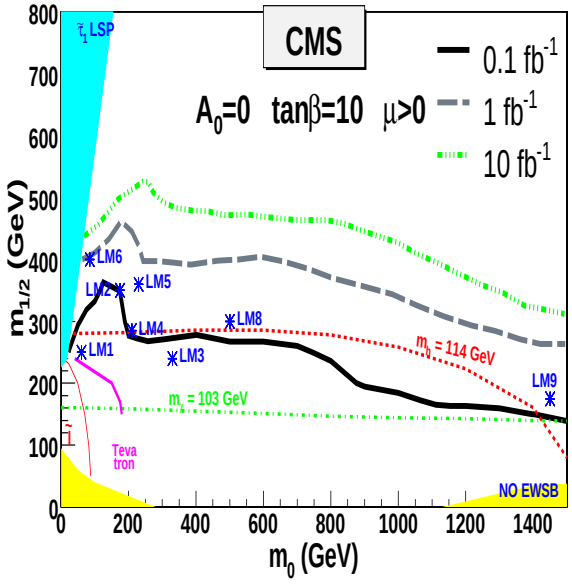

Figure 5: 5σ discovery contours for luminosities between 0.1 and 10 fb^{-1} at $\tan\beta = 10$ obtained by taking into account of the systematic uncertainties on the background in the significance.

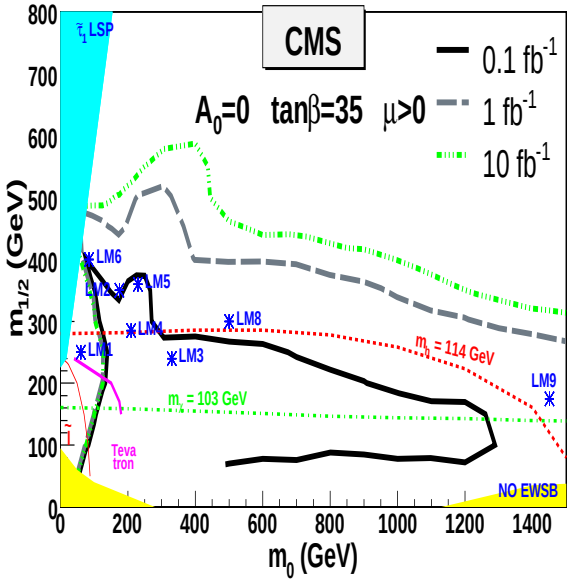

Figure 6: 5σ discovery contours for luminosities between 0.1 and 10 fb^{-1} at $\tan\beta = 35$ obtained by taking into account of the systematic uncertainties on the background in the significance.

For this study, a 40 fb^{-1} mSUGRA sample was generated at the LM2 test point with ISAJET 7.69 and PYTHIA 6.225 then simulated and reconstructed with FAMOS.

4.1 Fitting the invariant mass distributions

The extraction of the end-point is complicated by the presence of combinatorial background due to multiple τ and jet candidates. This combinatorial background is responsible for distorting and extending the invariant mass distributions far beyond the position of the end-point. Therefore, understanding the contribution of the combinatorial background is critical to this analysis in particular its behavior near the tail of these distributions.

To minimize the amount of combinatorial background, the building blocks of the invariant mass distributions are chosen such that:

- for the τ candidates:

  The two τ's produced in the $\tilde{\chi}_2^0$ cascade decay having opposite charges, only pairs of opposite charge τ's are allowed. Furthermore, only hadronic τ's are considered as large rate of leptons faking τ's may arise from other $\tilde{\chi}_2^0$ leptonic decays (This is not the case at the LM2 test point where the $\tilde{\chi}_2^0$ decay rate to $\tilde{\tau}$ is close to 96%)

- for the jet candidates, only the two most energetic jets are considered.

  The quark-jet produced through $\tilde{q} \rightarrow q\tilde{\chi}_2^0$ decay, used by the end-point technique, is always very energetic due to the large mass difference between the $\tilde{q}$ and the $\tilde{\chi}_2^0$. This mass difference is in particular larger than the one between the $\tilde{q}$ and the $\tilde{g}$. Since $\tilde{q}$ or $\tilde{g}$ are produced in pairs, this quark should be found among the two most energetic jets of the events. At the LM2 test point, 75% of the quark produced by the decay of the $\tilde{q}$ are found among those two jets.

Even if the above requirements minimize the combinatorial background, an important fraction still remains due to the use of the two jets and the multiple τ candidates either fake or real (depending on the SUSY cascades, up to 5 τ's may be produced). To estimate and ultimately remove the contribution of the remaining combinatorial background, invariant mass distributions are built using only combinations of τ's and jets which cannot be associated to any specific physics process.

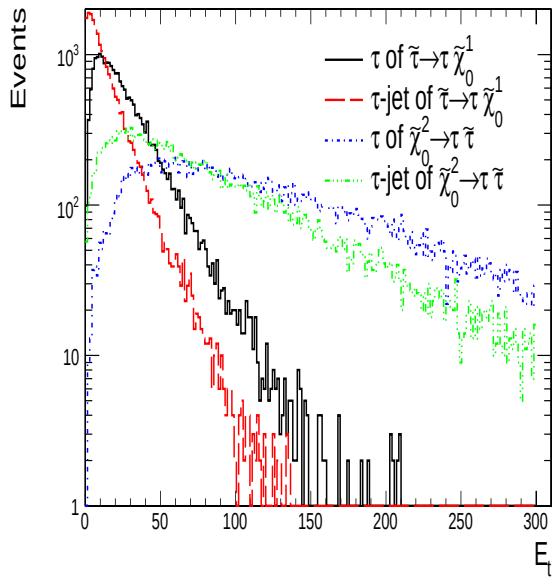

Figure 7: Transverse energy of the two τ's, as well as their detected detected product (τ-jet) τ's, produced in $\tilde{\chi}_2^0$ cascade.

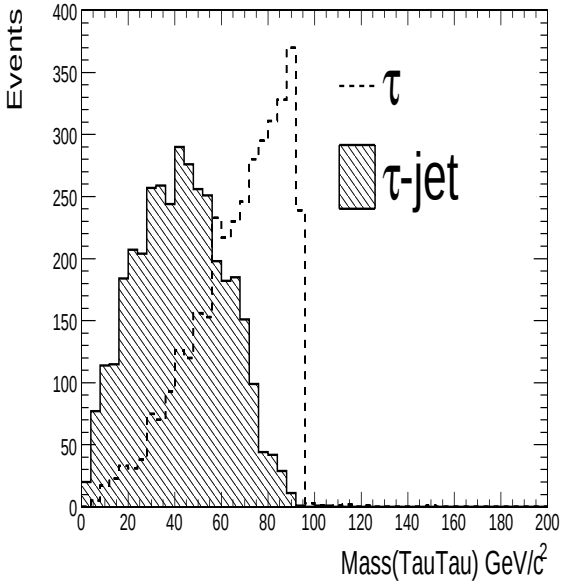

Figure 8: Di-τ invariant mass obtained at generator level with τ and with only visible τ decay products (τ-jet).

The estimation of the combinatorial background proceeds as follows:

- For τ pairs, only same charge combinations are allowed.

  This ensures that the resulting invariant mass is built with uncorrelated τ's and cannot be related to a same cascade. Its shape is identical to the combinatorial background found in the opposite charge di-τ sample since such combination occurs independently of the charge of the τ. However at the LM2 test point double charginos productions leads more often to final states with two opposite charge τ's than same charge τ's. However this excess is found to be negligible.

- For τ and jet combinations, one jet is taken randomly from the two most energetic jets of a different event.

  This ensures that combination of τ's and jets are strictly uncorrelated. In order to have the same amount of combinatorial background, all τ combinations (both with same and opposite charge τ's) are used with the jet. The combinatorial background associated to these combinations comes from wrong di-τ associations with a correct jet, true di-τ associations with a wrong jet or wrong di-τ associations with a wrong jet.

The distributions of the combinatorial background are fitted using a function of the form $(\alpha x)^{\,i} \exp\left[-\beta(\gamma x)^j\right]$. This function was found to give a good description of the various combinatorial background distributions. An example is shown in figure 9 for the di-τ invariant mass distribution where a χ^2 per degree of freedom of 0.6 was obtained.

The contribution from the combinatorial background is removed from the di-τ invariant mass distribution by subtracting the corresponding fitted distribution. The resulting distribution (residual) is shown in figure 10 (full circle). This one is in good agreement with the reconstructed di-τ invariant mass obtained with only $\tilde{\chi}_2^0$ decays.

Although, the end-point could easily be extracted from that distribution with good precision, this is not necessarily the case for the other invariant mass distributions. Furthermore, since the formulae giving the sparticle masses are function of the differences between the various end-points, it is mandatory to have the exact same treatment for all the invariant mass distributions to not introduce any bias in the procedure.

For these reasons, instead of just subtracting the fitted combinatorial background from the invariant mass distribution, the whole invariant mass distribution itself is fitted by the sum of the function describing the combinatorial background where the parameters are fixed to the value found in the combinatorial background fit, plus a log-normal term (equation 1) which is found to describe well the upper tail of the invariant mass distributions

associated to $\tilde{q} \rightarrow q\tilde{\chi}_2^0$ cascades. Figure 10 (dashed line), shows the log-normal term with parameters fixed to the values obtained from the fit of the invariant mass distribution shown in figure 9.

$$P(x) = Ke^{-\frac{1}{2\sigma^2}\ln^2(\frac{x-\theta}{\mu})} \tag{1}$$

As the log-normal distribution has a tail which goes to infinity, one has to decide where to truncate the distribution to find the position of the end-point. This information is obtained from the residual of the di-τ invariant mass which agrees very well with the log-normal distribution (figure 10). The position of that end-point E_0 is then defined as the position of the last observed point from the residual (here 95 GeV). The position of this observed end-point E_0 is translated in terms of probability of the log-normal distribution (equation 2) which is expressed in terms of a fraction δ of the maximum probability $P_{\max}$ of the log-normal distribution. That fraction was found to be around 0.05. Since these log-normal distributions are used in the fits of all the invariant mass distributions, their δ parameters are kept identical in all the invariant mass fits as well as for all the SUSY samples which are studied. This ensure a completely identical treatment of all the invariant mass distributions.

Since the place of the starting end-point E_0 (and hence value of the δ parameter) is related to the resolution of the di-τ invariant mass For the mass measurement, a systematic uncertainty due to the choice of the δ parameter is taken into account by varying the value of the δ parameter such that E_0 is varied by about twice the energy resolution.

The case of the di τ invariant mass is shown in figure 10 together with the true invariant mass distribution and the resulting signal function which is seen to reproduce well the upper tail of the true invariant mass distribution. Using the log-normal term the end-point is found to be 95 ± 3 GeV.

$$P(E_0) = \delta P_{\max} = Ke^{-\frac{1}{2\sigma^2}\ln^2(\frac{E_0-\theta}{\mu})} \text{and } P(x) = Ke^{-\frac{1}{2\sigma^2}\ln^2(\frac{x-\theta(\delta,E_i)}{\mu})} \tag{2}$$

4.2 End-point extraction and mass measurement

The full fitting procedure used here to extract the SUSY mass spectrum proceeds in several steps:

In a first step, $m(\tau_1\tau_2)$ and $m(\tau_1 q) + m(\tau_2 q)$ are fitted following the procedure described in the above section, their respective end-points are then extracted (the measured end-points are found in table 2. The fits of both signal and combinatorial background are shown in figures 9 and 11 for $m(\tau_1\tau_2)$ and $m(\tau_1 q) + m(\tau_2 q)$ invariant mass distribution, respectively. Their respective log-normal fit and residual are shown in figure 10 and 12.

Events with invariant mass larger than the measured end-points are considered as combinatorial background and removed before extracting the remaining end-points.

This procedure has the advantage of stabilizing the fitting procedure and facilitates the finding of the remaining end-points. The resulting $m(\tau_1 q)$, $m(\tau_2 q)$ and $m(\tau_1\tau_2 q)$ invariant mass distributions are fitted using the procedure described in section 4.1 The measured end-points are summarized in table 2. Fits to both signal and combinatorial background distributions are shown in figures 13, 15 and 17. The log-normal term of the fits as well as the residuals are shown in figures 14, 16 and 18. They are in good agreement with the tails of the reconstructed invariant masses obtained with only $\tilde{q} \rightarrow q\tilde{\chi}_2^0$ decays.

With these end-points, it is possible to estimate the mass of the sparticles involved in the cascade decay [15]. However, several hypotheses depending on the sparticle mass hierarchy are possible. At the LM2 test point, two hypotheses returns valid mass spectra. The case where $2m_{\tilde{\tau}}^2 > m_{\tilde{\chi}_2^0}^2 + m_{\tilde{\chi}_1^0}^2 > 2m_{\tilde{\chi}_2^0}^2 m_{\tilde{\chi}_1^0}^2$ (case 1) and $m_{\tilde{\chi}_2^0}^2 + m_{\tilde{\chi}_1^0}^2 > 2m_{\tilde{\chi}_2^0}^2 m_{\tilde{\chi}_1^0}^2 > 2m_{\tilde{\tau}}^2$ (case 2) which corresponds to the mass hierarchy of the LM2 test point. The values for the sparticle masses calculated for the two valid hypotheses are shown together with the measured end-point in table 2.

An attempt of chosing between the two solutions is achieved by checking the consistency of the two mass spectra with the end-point E_5 of the invariant mass distribution $m(\tau_1 q) + m(\tau_2 q)$ [16] which can be written in terms of sparticle masses as:

$$E_5 = (m(\tau_1 q) + m(\tau_2 q))^{\max} = \frac{1}{M_{\tilde{\chi}_2^0}}\sqrt{M_{\tilde{q}}^2 - M_{\tilde{\chi}_2^0}^2}[\sqrt{M_{\tilde{\chi}_2^0}^2 - M_{\tilde{\tau}}^2} + \sqrt{M_{\tilde{\tau}}^2 - M_{\tilde{\chi}_1^0}^2}] \tag{3}$$

The most probable mass hypothesis is then chosen as the one for which E_5 calculated with the above formula is the closest to the measured one. The measured end-point was found to be $780 \pm 20(\mathrm{stat})$ GeV while the calculations for the case 1 and case 2 mass hierarchy yield to $815 \pm 26(\mathrm{stat})$ GeV and $765 \pm 30(\mathrm{stat})$ GeV respectively. The second hypothesis, which corresponds to the LM2 mass hierarchy (table 3) is closer to the measured end-point value.

The systematic uncertainties on the mass measurements are estimated by varying independently both τ and jet transverse energies within their energy scales. A systematic uncertainty is also taken into account for the choice of the δ parameter. All contributions are added in quadrature. The resulting sparticle masses are shown together with their theoretical values for the LM2 test point at 40 fb^{-1} in table 3, They are in good agreement with the sparticle mass values as generated in the Monte Carlo.

Table 2: End-point obtained with the log-normal fit together with sparticle masses measured with the end-point technique for LM2 for integrated luminosities around 40 fb^{-1}. Only statistical uncertainties are shown.

End-points (GeV)	case 1 (GeV)	case 2 (GeV)
$m(\tau_1\tau_2)^{\max} = 95 \pm 3$	$M(\tilde{\chi}_1^0) = 213 \pm 14$	$M(\tilde{\chi}_1^0) = 147 \pm 23$
$m(\tau_1 q)^{\max} = 559 \pm 11$	$M(\tilde{\chi}_2^0) = 337 \pm 17$	$M(\tilde{\chi}_2^0) = 265 \pm 10$
$m(\tau_2 q)^{\max} = 298 \pm 7$	$M(\tilde{\tau}) = 310 \pm 17$	$M(\tilde{\tau}) = 165 \pm 10$
$m(\tau_1\tau_2 q)^{\max} = 596 \pm 12$	$M(\tilde{q}) = 839 \pm 19$	$M(\tilde{q}) = 763 \pm 33$
$E_5^{meas} = 780 \pm 20$	$E_5^{calc} = 815 \pm 26$	$E_5^{calc} = 765 \pm 30$

Table 3: sparticle masses measured with end-point method for LM2 together with theoretical value

	LM2 test point	
	measured	theory
$M(\tilde{\chi}_1^0)$ (GeV)	$147 \pm 23(\mathrm{stat}) \pm 19(\mathrm{sys})$	138.2
$M(\tilde{\chi}_2^0)$ (GeV)	$265 \pm 10(\mathrm{stat}) \pm 25(\mathrm{sys})$	265.5
$M(\tilde{\tau})$ (GeV)	$165 \pm 10(\mathrm{stat}) \pm 20(\mathrm{sys})$	153.9
$M(\tilde{q})$ (GeV)	$763 \pm 33(\mathrm{stat}) \pm 58(\mathrm{sys})$	753-783 (light $\tilde{q}$)

5 Conclusions

In this note, the discovery potential of $\tilde{\tau}$ production through the mSUGRA cascade decay has been investigated, if the nature favors such a model, a discovery could be possible with only few hundreds of pb^{-1}.

Using a 40 fb^{-1} LM2 sample, we show that a measurement of the SUSY mass spectra and in particular of the mass of the $\tilde{\tau}$ can be performed with a precision of less than 30 GeV.

6 Acknowledgments

The authors would like to thank Simone Gennai, Sasha Nikitenko, Luc Pape, Albert de Roeck and Maria Spiropulu for the careful reading of that note and the useful comments and suggestions they made through out the process on the analysis. The authors are more particularly grateful to Maria Spiropulu for her support and interest in the analysis and helping us improving the content of the note.

References

[1] H. P. Nilles, Phys. Reports, 110 (1984) 1; P. Nath *et al. Applied N=1 Supergravity* World Scientific Singapore, 1984; S. P. Martin *Perspectives on supersymmetry* World Scientific Singapore, 1998.

[2] M. Battaglia *et al.* , Eur. Phys. J.C22, 535-561, 2001; M. Battaglia *et al.* , Eur. Phys. J.C33, 273-293, 2004.

[3] J. Pumplin *et al.*, JHEP 07:012, 2002.

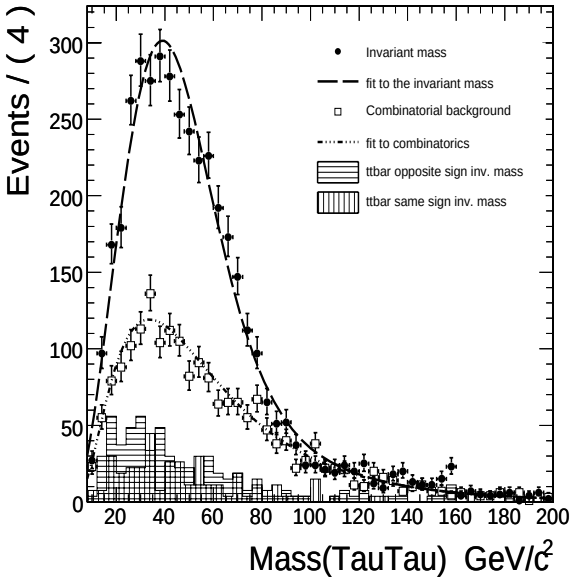

Figure 9: Di-τ Invariant mass distributions for signal and combinatorics together with the fitting functions for LM2.

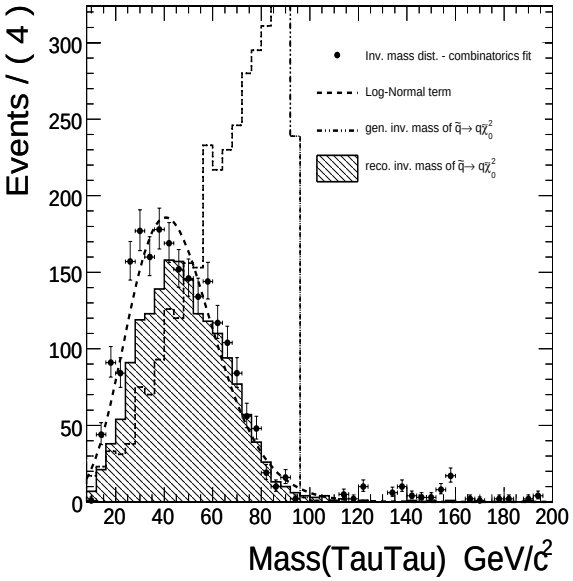

Figure 10: Di-τ invariant mass distribution of the signal obtained after subtracting the combinatorial fit together with the log-normal term used in the invariant mass fit.

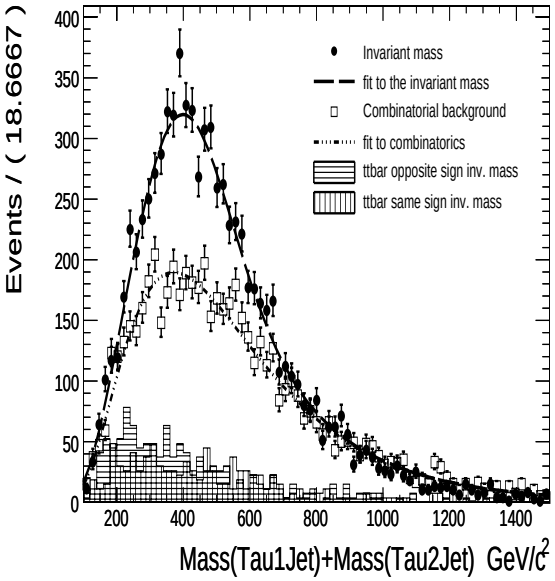

d

Figure 11: Distributions of $m(\tau_1 q) + m(\tau_2 q)$ for both signal and combinatorics together with the fitting functions for LM2.

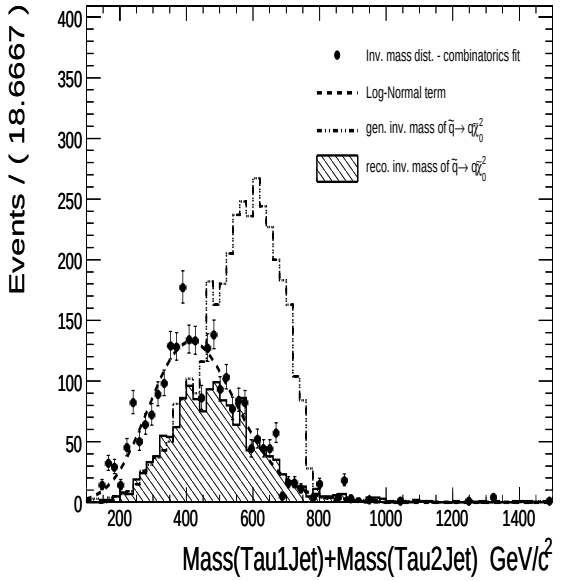

Figure 12: $m(\tau_1 q) + m(\tau_2 q)$ invariant mass distribution of the signal obtained after subtracting the combinatorial fit together with the lognormal term used in the invariant mass fit.

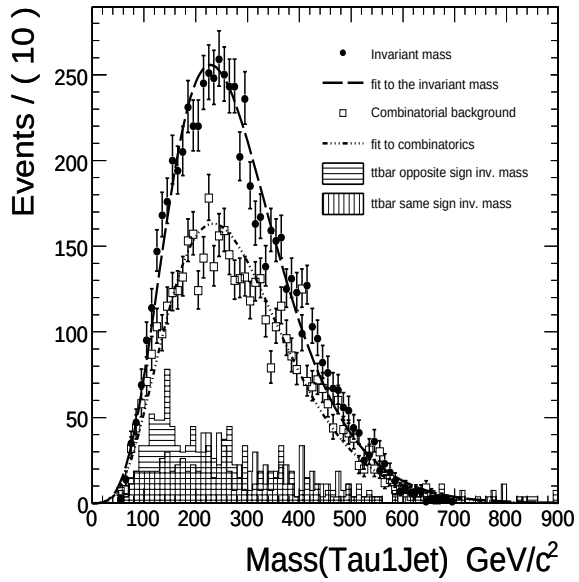

Figure 13: Distributions of $m(\tau_1 q)$ for both signal and combinatorics together with the fitting functions for LM2.

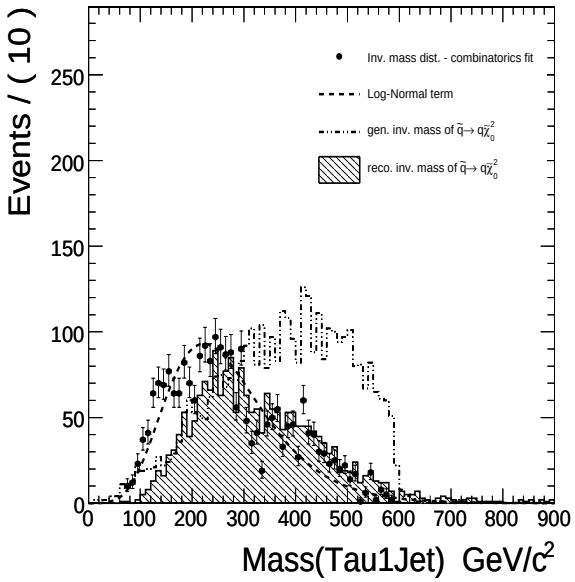

Figure 14: $m(\tau_1 Q)$ invariant mass distribution of the signal obtained after subtracting the combinatorial fit together with the log-normal term used in the invariant mass fit.

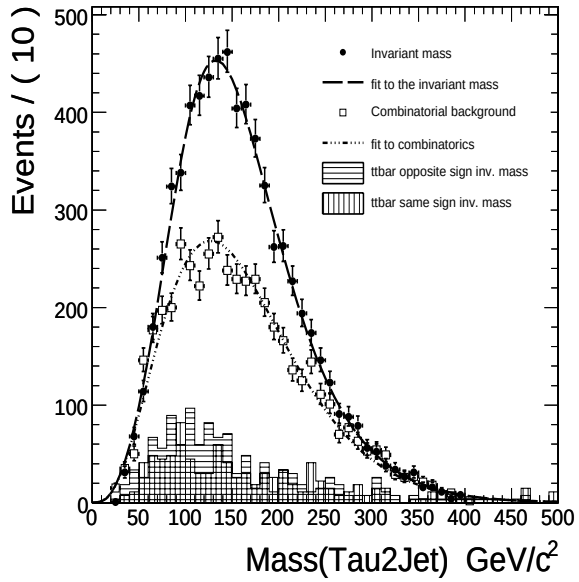

Figure 15: Distributions of $m(\tau_2 q)$ for both signal and combinatorics together with the fitting functions for LM2.

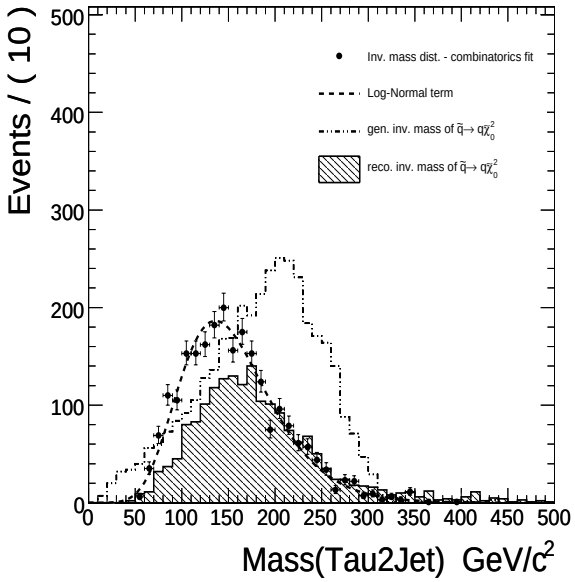

Figure 16: $m(\tau_1 q)$ invariant mass distribution of the signal obtained after subtracting the combinatorial fit together with the log-normal term used in the invariant mass fit.

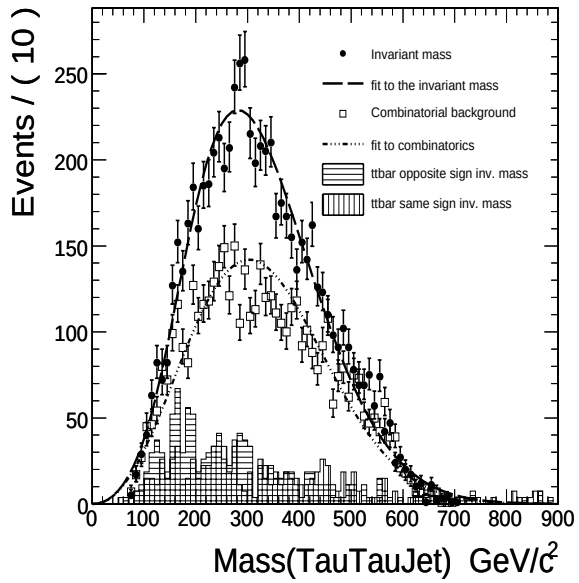

Figure 17: Distributions of $m(\tau_1\tau_2 q)$ for both signal and combinatorics together with the fitting functions for LM2.

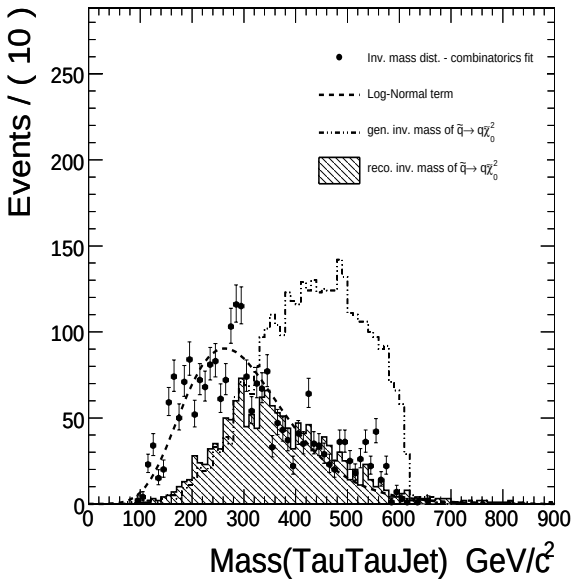

Figure 18: $m(\tau_1\tau_2 q)$ invariant mass distribution of the signal obtained after subtracting the combinatorial fit together with the log-normal term used in the invariant mass fit.

[4] H. Baer *et al. "ISAJET 7.69: A Monte Carlo Event Generator for pp, $\bar{p}p$, and e^+e^- Interactions"*, hep-ph/0312045.

[5] T. Sjostrand *et al.,"PYTHIA 6.2: Physics and manual"*, hep-ph/0108264.

[6] The CMS collaboration, OSCAR: CMS Simulation Package Home Page, http://cmsdoc.cern.ch/oscar

[7] The CMS Collaboration, CMS OO Reconstruction , http://cmsdoc.cern.ch/orca.

[8] The CMS Collaboration, D. Acosta *et al.,"CMS Physics TDR Volume1, Section 2.6: Fast simulation"*, CERN/LHCC 2006-001 (2006) 55.

[9] A. Heister *et al. "Measurement of jets with the CMS detector at the LHC"*, **CMS Note 2006/036**.

[10] Haifeng Pi *et al. "Measurement of Missing Transverse Energy with the CMS detector at the LHC"*, **CMS Note 2006/035**.

[11] V. Konoplianikov *et al. "Jet Calibration using gamma+jet events in the CMS detector"*, **CMS Note 2006/042**.

[12] S. Gennai *et al. "Tau jet reconstruction and tagging at high level trigger and off-line"*, **CMS Note 2006/028**.

[13] S. Bityukov *et al., "Program for evaluation of significance, confidence intervals and limits by direct calculation of probabilities"*, Proceeding of PhyStat 2005 (2005)

[14] V. Bartsch and G. Quast, *" Expected signal observability at future experiments"*, **CMS Note 2005/004**; R. Cousins *et al., "Detection of Z' gauge bosons in the dimuon decay mode in CMS"*, **CMS Note 2005/002**.

[15] B. K. Gjelsten *et al.*, JHEP 0412:003,2004

[16] F. Heinemann, *The discovery potential of the second-lightest neutralino in mSUGRA in the tau-channel at high tan(b) at the LHC*, hep-ex/0406056